**THESIS FOR THE DEGREE OF MASTER OF SCIENCE**

# Genetic Mapping and Characterization of a Stunted Growth Mutant in Rice (*Oryza sativa* L.)

**BY**

**HYE KYUNG SON**

**AUGUST, 2018**

**MAJOR IN CROP SCIENCE AND BIOTECHNOLOGY**
**DEPARTMENT OF PLANT SCIENCE**
**THE GRADUATE SCHOOL OF SEOUL NATIONAL UNIVERSITY**

# Genetic Mapping and Characterization of a Stunted Growth Mutant in Rice (*Oryza sativa* L.)

**HYE KYUNG SON**

## ABSTRACT

We identified a stunted growth mutant from a *japonica* rice cultivar, Samgwang, treated with *N*-methyl-*N*-nitrosourea (MNU). The mutant showed dwarf, narrow leaf and sterile panicle. The retardation growth of the mutant initiated at the seedling stage and became severe at the reproductive stage. The plant height was reduced by 34% compared to that in wild type and showed significantly decreased first four internode length. The width of flag leaf was reduced by 46% in mutant compared with wild type. Anatomical analysis of leaves suggested that less number of the vascular bundles and epidermal cells caused narrow leaf. Also, mutant plants showed low pollen viability and complete sterility. Genetic analysis indicated that the mutation was controlled by a single recessive gene. The $F_2$ generations of a cross between mutant and Milyang23 were used for mapping. Candidate region was detected to a short arm of chromosome 5 near the marker S05000 and S05032 via BSA method. The mutant was fine-mapped

at an interval of 84kb flanked by the markers NC0501.48 and NdC0501.56. Sequencing of the region identified that the mutant carries 11bp insertion in the third exon of *LOC_Os05g03550,* a gene which contains two SANT domains related to histone deacetylation. The insertion led to premature stop codon in coding sequence. Quantitative RT-PCR analyses revealed that in wild type, the transcripts of *LOC_Os05g03550* were constitutively expressed during whole growth period with gradual increase. Accordingly, a novel gene that cause inhibition of plant growth was isolated and the results may provide a basis for functional studies of the gene associated with growth and development of rice.

**Keyword:** Rice, Stunted growth, Dwarfism, Narrow leaf, Sterility, Fine mapping, SANT domain.

**Student Number:** 2016-25286

# CONTENTS

# LIST OF TABLES

# LIST OF FIGURES

# LIST OF ABBREVIATIONS

| | |
|---|---|
| BSA | Bulked segregant analysis |
| BLAST | Basic Local Alignment Search Tool |
| CAPS | Cleaved Amplified Polymorphic Sequences |
| cDNA | complemantary DNA |
| DBD | DNA binding domain |
| dCAPS | Derived Cleaved Amplified Polymorphic Sequences |
| DNA | Deoxyribonucleic acid |
| HAT | Histone acetylase |
| HDAC | Histone deacetylase |
| InDel | Insertion/deletion |
| $I_2$-KI | Iodine-potassium iodide |
| LC2s | the flanking stomatal row long cells |
| MNU | *N*-methyl-*N*-nitrosourea |
| N-CoR | Nuclear receptor co-repressor |
| PCR | Polymerase chain reaction |
| PWR | POWERDRESS |
| qRT-PCR | Quantitative real time PCR |
| SANT | SWI3/ADA2/N-CoR/TFIII-B |
| SMRT | Silencing mediator for retinoic acid and thyroid receptor |
| SNP | Single nucleotide polymorphism |
| STS | Sequence tagged site |

# INTRODUCTION

Rice (*Oryza sativa* L.) is one of the most important cereal crops world-wide. It is one of the main purposes to develop ideotype lines described as a mixture of characteristics favorable for photosynthesis, growth, and grain production in rice breeding (Donald, 1968). For example, the semi-dwarf varieties were less prone to lodging in adverse weather conditions and also responded better to nitrogen fertilizers by increasing grain yield (David and Otsuka, 1994). Rice production is correlated with multiple factors, such as tiller number, grain number per panicle, grain size, and plant height. Plant height is important trait in plant architecture since it contributes advantage to higher photosynthetic efficiency and development of other organs. Genes regulating plant architecture have been categorized into three classes, involving in hormone metabolism and signaling, transcription and other regulatory factors, and cell cycle regulation (Busov et al., 2008). These genes are essential for normal plant growth condition and directly influence to agronomic values. Therefore, numerous mutants have been studied for plant morphogenesis and differentiation, and their causal genes have been cloned (Itoh et al., 2005).

During the last two decades, many studies were progressed to find out the mechanism of regulating plant height. Genes associated with gibberellin (GA), brassinolide (BR), strigolactone (SL) biosynthesis and signal

transduction were found to highly contribute to dwarf phenotype. Apart from genes related to hormones, *OsKinesin-13A* (Deng et al., 2015), *OSH15* (Sato et al., 1999), *OsGSP1* (Banerjee and Maiti, 2010) and *DTH8* (Wei et al., 2010) were also found to affect in plant height.

Many dwarf mutants are associated with other organ development as well. For example, The *TRYPTOPHAN DEFICIENT DWARF1* (*TDD1*) gene located on chromosome 4 encodes a protein homologous to the anthranilate synthase β-subunit working on upstream of Trp-dependent IAA biosynthesis. The *tdd1* mutant shows pleiotropic phenotypes: dwarfing, narrow leaves, short roots and abnormal flowers (Sazuka et al., 2009). The *DWARF AND DEFORMED FLOWER3* (*DDF3*) gene is located on chromosome 7 and the *ddf3* mutant exhibits dwarfism, increased tillers and reduced fertility (Wang et al., 2018). *DEFORMED FLORAL ORGAN1* (*DFO1*) which encodes a nuclear-localized protein was identified as a rice epigenetic repressor by reducing expression of *OsMADS58*. The *dfo1* mutant lead to a small stature and defects in floral organ identity (Zheng et al., 2015).

In addition, several rice genes which lead to specific narrow leaf phenotype were cloned from mutants. The *COW1/NAL7* gene located on the short arm of chromosome 3 encodes a YUCCA protein associated with auxin biosynthesis. This phenotype showed significant difference in leaf width but not in leaf length compared to wild type (Fujino et al., 2008; Woo et al., 2007). The *NAL1* located on chromosome 4 encodes a plant specific protein

related to polar auxin transport. The *nal1* mutant exhibits narrow leaves and also significantly shorter leaves compared to wild type (Qi et al., 2008). The *NAL9* located on chromosome 3 encodes ATP-dependent Clp protease proteolytic subunit. The *nal9* mutant displays narrow leaf phenotype along with more tillers and light green leaves (Li et al., 2013). The *NRL/ND1* located on chromosome 12 encodes cellulose synthase-like proteins D4 (OsCslD4). This mutant leads to reduced leaf length and width (Hu et al., 2010; Li et al., 2009; Wu et al., 2010).

Despite the importance of growth aspects, little is known about molecular mechanism controlling integrative development of rice due to its complicated process associated with many genes. Regarding to previous studies, transcription regulation has observed as a critical process in diverse plant growth aspects. Genes encoding basal transcription regulating factors have an important role to recruit a protein complex that enables chromatin modification and/or remodeling to switch its target gene on, and induce a specific developmental output. Epigenetic modification is an important gene regulatory mechanism in eukaryotic organisms. This is another level of genetic control likewise DNA sequence change. Posttranslational modifications of histone including acetylation, methylation, phosphorylation and ubiquitination play essential roles in genome stability, plant development and stress responses and are closely related to gene expression (Struhl, 1998).

SANT domain-containing proteins are one of the transcription regulating factors associated with histone modification. Binding to histone tails and establishing a complex with transcription factors are known as predominant functions of SANT domain-containing protein. SANT domain was first discovered in nuclear receptor co-repressor (N-CoR) (Aasland et al., 1996). In N-CoR amino acid sequence, two copies of ~50-residue motif spaced 129 residues apart were observed and these were matched with three different proteins in yeast: SWI3 and ADA2 (basal or activated transcription complexes), TFIIIB (component of RNA polymerase III initiation complex). Therefore, it was named as SANT(SWI3/ADA2/N-CoR/TFIII-B) domain. This domain was first described as a putative DNA binding domain (DBD) because of sequence analogy and structural similarity with DBDs of Myb (Aasland, 1996). However, based on biochemical analyses and electrostatic modelling, it was clearly proved that that the SANT domains function as histone-binding modules that is different from DNA binding (Boyer et al., 2004).

Nuclear receptor has the unique ability to directly bind to DNA and regulate the expression of adjacent gene by forming a complex with coregulators (coactivators and corepressors), and other proteins. Corepressor binds to un-ligand nuclear receptor and gather histone deacetylases (HDACs). This complex represses gene transcription by enhancing the association of histones to DNA (Watson et al., 2012). In contrast, binding of

ligand to nuclear receptor induces coactivator protein binding. Coactivators often have histone acetyltransferase (HAT) activity, and promotes gene transcription by attenuating histone and DNA complex. Among nuclear receptor corepressors, silencing mediator for retinoic acid and thyroid receptor (SMRT) and nuclear receptor co-repressor (N-CoR) are most well studied. In contrast to the comprehensive study of SANT domain-containing proteins in yeast and animals, the function of SANT domain-containing proteins in plants remains unclear.

Recently, in Arabidopsis, the SANT domain-containing protein, POWERDRESS, which has predominant role in HDAC function was detected. The *pwr* mutant exhibited broad spectrum of developmental defects in leaf and floral formation, transition of developmental stages and senescence, which indicates that *PWR* affected various biological processes with serious effect on plant growth and development (Chen et al., 2016; Kim et al., 2016; Suzuki et al., 2018; Yumul et al., 2013). However, studies for SANT-domain containing protein in rice has not been informed yet.

In the present study, the main purpose was to isolate a novel gene related to stunted growth, and attain a new rice germplasm. Although several genes have been reported to control various organ development with plant height, it still remains unclear. To gain further insight into the genetic regulation in plant development, we identified and characterized the chemical treated mutant which exhibited multiple defects during overall growth period,

including smaller plant stature, abnormal leaf shape and spikelet sterility. With genetic mapping, we determined a candidate gene, *LOC_Os05g03550* which has a pair of SANT domains that presented high sequence similarity with those of other SANT domain-containing proteins described above. In addition, phenotypes of the stunted growth mutant showed great consistency with those of the *pwr* mutant in Arabidopsis. A BLAST search of LOC_Os05g03550 showed no homologs in rice. In light of these findings, our result will provide an important starting point for further analysis of SANT domain-containing proteins regulating development in rice.

# MATERIALS AND METHODS

## Plant materials and growth conditions

The mutant was induced by treatment of *N*-methyl-*N*-nitrosourea (MNU) from the *japonica* cultivar Samgwang. The mutant was crossed with Samgwang, a *japonica* cultivar, and Milyang23, a Korean *Tongil*-type cultivar derived from cross of *japonica*/*indica* and similar to genetic background of *indica*. For genetic analysis, mutant was crossed with Samgwang to construct $F_1$ and $F_2$ generations. A mapping population of 840 $F_2$ – $F_4$ progenies was generated from a cross between mutant and Milyang23. The parent plants and $F_1$ – $F_3$ progenies were cultivated in the paddy field of Experimental Farm of Seoul National University (Suwon, Korea) by conventional methods with natural long day conditions. The $F_4$ plants of a cross between mutant and Milyang23 and plants for RNA extraction were grown in greenhouse of Experimental Farm of Seoul National University.

## Measurement of morphological traits

Morphological traits were measured to compare differences among wild type and mutant during the maturation stage. Scored traits included the plant height, culm length, panicle length, number of panicles per plant, length and

width of leaf blade, internode length, panicle exsertion and heading date. For all these traits, we sampled 10 plants in each wild type and mutant. The main culm panicle of each plant was chosen for measurement. The plant height was measured from the surface of the ground to the leaf tip. The width of leaf blade was measured at the widest part of each leaf blade. The obtained data were analyzed for significance level by an unpaired *t*-test. If $P<0.05$, it was considered that there is a significant difference in phenotype. GraphPad Prism7 program (GraphPad Software, USA) was used for implementing an unpaired *t*-test and graph construction.

**Anatomical analysis**

Paraffin-embedded leaf sections were prepared for further investigation of the leaf phenotype. Three plants in each wild type and mutant at the booting stage were used and in each plant, leaves second to the top were acquired. The midpoint of leaves cut in 1cm length were collected and fixed in formalin-acetic-alcohol (FAA) fixative buffer (3.7% formaldehyde, 5% acetic acid, 50% ethanol) at 4℃ overnight. The samples were dehydrated with 50-85% graded ethanol solution series for 2hrs each at room temperature and the samples were soaked in 100% ethanol overnight. After dehydration, samples were infiltrated with ethanol and xylene substitute, histoclear, mixture for 2hrs at room temperature as follows: ethanol/histoclear (3:1, v:v), ethanol/histoclear (1:1, v:v), ethanol/histoclear

(1:3, v:v), and pure histoclear overnight. For paraffin infiltration, Paraplast® (Sigma, USA) was gradually added to histoclear solution. Samples were infiltrated with histoclear and paraffin mixture for 2hrs in an oven at 55℃ as follows: histoclear/paraffin (3:1, v:v), histoclear/paraffin (1:1, v:v), histoclear/paraffin (1:3, v:v), and pure paraffin overnight. Next, the paraffin-infiltrated samples were embedded in a block and sectioned at a thickness of 10um using a rotary microtome (Thermo Fisher Scientific, USA). Transverse and longitudinal sections were mounted on clean glass slides coated with distilled water and dried at 42℃ for 1 day. The dried sections were deparaffinized by immersing them in 100% xylene for 20 min and in a series of increasing ethanol concentration for 2 min. Then, the specimens were immersed in distilled water for 2 min. Next, the specimens were stained with 0.1% Toluidine Blue O solution (TBO) for 30 sec and rinsed briefly with distilled water. For dehydration, the specimens were soaked in a series of increasing ethanol concentration for 2 min and cleared with xylene for 10 min. Finally, the specimens were mounted with Canada balsam and air dried overnight. The specimens were observed under a microscope (Olympus, Japan). For analysis of cell size, epidermis of abaxial side of leaf blade was observed. Among epidermal cells, flanking stomatal row long cells (LC2s) were used for determination of cell length and width. The image of cell was acquired at 40X and 100X magnification by eXcope digital camera (DIXI Science., Korea). The length and width of individual

cells were measured in eXcope program. The values obtained from six replicates were analyzed by an unpaired *t*-test to compare difference between wild type and mutant, and $P<0.05$ indicated statistical significance. GraphPad Prism7 program (GraphPad Software, USA) was used for implementing an unpaired *t*-test and graph construction

**Investigation of pollen viability**

Pollen viability was examined by staining with 1% iodine-potassium iodide ($I_2$-KI) solution. Generally, for normal dehisced anthers of wild type, pollen grains were directly collected at anthesis on a slide by tapping anthers and for indehiscence anthers of mutant, pollen grains were manually squashed onto a slide and released pollen grains were observed. However, for exact calculation of pollen viability, in both wild type and mutant, six anthers were extracted before anthesis and squashed manually, followed by the addition of a drop of 1% $I_2$-KI solution. The number of stained pollen grains in each individual was immediately countered under microscope. The pollen was considered viable when the pollen wall was intact and the content evenly stained. For the test, three plants for each wild type and mutant type were used, and five spikelets per plant were taken.

**Statistical and genetic analysis**

For genetic analysis, $F_2$ generations were developed from a cross between mutant and Samgwang. The number of wild type and mutant type plants in $F_2$ generations were counted in maturing stage. Chi-square tests were performed to determine whether goodness-of-fit indicated conformity to a ratio of 3:1 using Statistical Analysis System (SAS) program (SAS institute, USA).

**Genetic mapping of the mutant gene**

$F_2$-$F_4$ generations derived from a cross between mutant and Milyans23, which included a total 840 plants, were used for mapping of the candidate gene locus. Genomic DNA was extracted from young leaves of each plants using the CTAB method. For bulked segregant analysis (BSA), ten wild type plants and ten mutant type plants were selected from $F_2$ population and equal amount to DNA were pooled into two bulks (Michelmore et al., 1991). BSA was performed with total 109 STS markers evenly distributed on the rice genome to find out the markers linked to the candidate gene. STS markers were previously designed by Crop Molecular Breeding Lab, Seoul National University (Chin et al., 2007). For further fine-mapping of the candidate region determined by BSA, new STS, CAPS, and dCAPS markers were developed with primer3 version 0.4.0 (http://bioinfo.ut.ee/primer3-0.4.0/) and dCAPS finder 2.0 (http://helix.wustl.edu/dcaps/) using

comparison of DNA sequences between *indica* and *japonica* rice (NCBI; https://www.ncbi.nlm.nih.gov/). KNJ8-Indel354 marker was previously designed by Yonemura et al. (2015). The information of primers used for fine mapping is listed in Table 1. Specific fragments from the mutant and wild type cultivar Samgwang were amplified by PCR.

**Analysis of candidate genes**

To identify the variation in the candidate region, whole genome sequencing of mutant was conducted using Illumina HiSeq 2500 sequencing, 250cycle PE lane, 10Gb. Mutant sequence reads were obtained and aligned to Nipponbare reference sequence to find out mutant SNP positions. The insertion of genomic fragment determined by sequencing result in the candidate region was confirmed by specifically designed primers (Table 1) for amplifying the insertion region in genomic DNA and cDNA. PCR products amplified from Samgwang and mutant were separated on 1.2% agarose gel and purified by Gel & PCR Purification kit (Inclone, Korea). Purified PCR products were ligated to pGEM-T Easy Vector (Promega, USA), followed by transformation into *E.coli* strain DH5α. Plasmid products purified by Plasmid Purification kit (Inclone, Korea) were sequenced with an ABI Prism 3730 XL DNA Analyzer (PE Applied Biosystems, USA) and aligned with CodonCode Aligner software (CodonCode Corporation, USA). Co-segregation test was performed to

confirm nucleotide insertion point with designed InDel marker (Table 1).

**RNA extraction and qRT-PCR analysis**

Total RNA was isolated from various rice organs including leaves, second internodes and young panicles of wild type and mutant at booting stage using RNAiso plus reagent (Takara Bio, Japan) according to the manufacturer's instructions. In case of leaves, RNA was extracted at seedling stage and vegetative stage after tillering as well as booting stage. The extracted RNA was treated with RNase-free Recombinant Dnase I (Takara Bio, Japan) to eliminate remaining genomic DNA. First-strand cDNA was synthesized with oligo(dT) primers and DNase-treated RNA using M-MLV reverse transcriptase (Promega, USA). A quantitative Real-time PCR (qRT-PCR) was performed using specific primers which amplify coding sequence and SYBR premix ExTaq (Takara, Japan) on CFX96$^{TM}$ Real-Time PCR system (Bio-Rad, USA) according to the manufacturer's instructions. In each experiment, three biological repeats each with three technical replicates were carried out. The relative expression level of each transcript were measured by ΔΔCt method after being normalized with *UBIQUITIN5* expression. The primers used in qRT-PCR are listed in Table 1.

**Amino acid sequence alignment**

The amino acid sequence of LOC_Os05g03550 protein was obtained from MSU database (http://rice.plantbiology.msu.edu/) and two SANT domain sequences were collected from BLASTP (https://www.ncbi.nlm.nih.gov/). Search for the conserved domain structure was performed in PHYRE2 Protein Fold Recognition Server (www.sbg.bio.ic.ac.uk/phyre2/). Multiple sequence alignment of the conserved domain was carried out with ClustalX (http://www.clustal.org/) and reformatted with BOXSHADE (http://www.ch.embnet.org/software/BOX_form.html). The information of the protein sequences used in multiple alignment was from Kim et al. (2016).

**Table 1. Information of primers used in this study**

| Primer name | Purpose | Forward primer (5'→3') | Reverse primer (5'→3') | Note |
|---|---|---|---|---|
| S05000 | Mapping | GCAGGCGATGATAAGGGTTA | CAGCACCTCAAGCGTCCTA | InDel |
| NdC0500.45 | Mapping | CGTTGTCGAGGGATTGGCCCG | AGGAGGCGCTCTACTTCCAC | dCAPS |
| NdC0500.6 | Mapping | TAACTGCGTTTTTGCAGTGG | AAGCCACGAATATCAGGAGATT | dCAPS |
| NdC0500.97 | Mapping | AAAGCTGGGCAATCTACCTC | TGCTGCAAGGCAAGAATCTA | dCAPS |
| NdC0501.24 | Mapping | GAGTCCCGACTCCAGGAACT | CATCAGACTCTGTGGTGGCG | dCAPS |
| NC0501.44 | Mapping | TGGTTACATTAAGGGCGATTT | TTGCACAAGGTGGAGTAGCA | CAPS |
| NC0501.48 | Mapping | CAGATGCCCACCTCTTCAAC | CTGGGCAGTAGAGCACAAGA | CAPS |
| NI0501.50 | Mapping | GGCACCACATCACATGAAAG | GAGCAACCGATCATCACAGA | InDel |
| NdC0501.51 | Mapping | GGAGTAGTGGCTTCGTAGGG | CTTTTGCCTCGTGCGACG | dCAPS |
| NdC0501.56 | Mapping | AGTGTTAGATCCGGCTGTGG | TACAGCGAGGAGGTGAGGAGT | dCAPS |
| NI0501.61 | Mapping | TGCTTCATCCTGTTCATAAAAATC | CGACGACACTGCTCAATTGTACT | InDel |
| NC0501.67 | Mapping | CAGCAAACGCACACGAATTA | TTCAGGCACCTGTGAGTACG | CAPS |
| NC0501.71 | Mapping | TCTAACGTTCGCCGTACTCC | CCAAGAACCGGATCTCTTCA | CAPS |
| NdC0502.0 | Mapping | CGTGAGGCCACACATCGAGAAGCCC | ACGACACCTCGCACGTTAC | dCAPS |
| NC0502.25 | Mapping | CCCATGAGTTTGGACTTTGG | TGATGGAGTTGAACCTGATGA | CAPS |
| NC0502.36 | Mapping | CCAGGCGATCTTTTGTTTCT | CGTTTACGAGCACTGGGAAT | CAPS |
| KNJ8-Indel354 | Mapping | ATGACACTTTGAAGGTCGTGTG | GCCTCCTAATCAGTTTCGTTGT | InDel |
| S05032 | Mapping | GGGGAAACTGTTCAAGAAGG | CCTCCCCCTCTGTCTGTTTT | InDel |
| NI0505.84 | Mapping | CAAAGTCTGAAGGCCCTGTT | CATCGACAATGACAAAAGATGC | InDel |

| S05054 | Mapping | CCACTCACCAAGCCCTAATC | AGAGCAGTGTTCAGCAAGCA | InDel |
|---|---|---|---|---|
| S4-I | sequencing | GAGCAACCGATCATCACAGA | ACAGCTTCCTTGCTACACCT | — |
| S2 | sequencing | ATCAATGGGATCACCCTCAA | ACGGCTATTACCGACAGG | — |
| S3 | sequencing | TCAAGATTGGACCGATCAGC | GGGAATCACCCATACACCAG | — |
| S4 | sequencing | TATGCCTGCCAAGACATCAG | TATTGCTGCGAACAGGAGTG | — |
| S5 | sequencing | TCAACTGAAGTGGCCATGAG | ATGCGGCATCACTTGATATG | — |
| qOsUbi5 | qRT-PCR | ACCACTTCGACCGCCACTACT | ACGCCTAAGCCTGCTGGTT | — |
| qEX1 | qRT-PCR | GGAGGATGTGCGACTTCTTT | CTGAGATCCGCTCTGTGATG | — |

# RESULTS

## Characterization of a stunted growth mutant

The stunted growth mutant was induced by treatment of *N*-methyl-*N*-nitrosourea (MNU) on a *japonica* rice cultivar, Samgwang. The mutant exhibited retarded growth in many aspects of plant development during the whole growth period. During the vegetative stage, mutant seedlings developed narrow leaves and reduced plant height compared to the wild type. This phenotype was distinguished as early as 21 days after sowing. The reduced stature of the mutant became severe proceeding to maturity. General agronomic traits were measured in Table2. In the reproductive stage, the mutant exhibited delayed flowering, spikelet sterility, and unfilled grains. As described, predominant morphological traits in mutant could be categorized into three aspects: dwarfism, narrow leaf and sterile spikelet.

First, the stunted growth mutant showed shorter plant height than that of wild type. The difference of plant height appeared from seedling stage, but it was observed more clearly from the late vegetative stage and achieved the maximum level in the reproductive stage (Figure.1-A, B). To compare the difference of plant height, we measured the plant height and length of internode in ripening stage. The plant height was reduced by 34% compared

to that of wild type, and showed significantly decreased first four internode lengths. From the upper most internode to the third internode in mutant, each length was reduced by 38%, 44% and 50% compared to the wild type, respectively (Figure.1-D, Figure. 2).

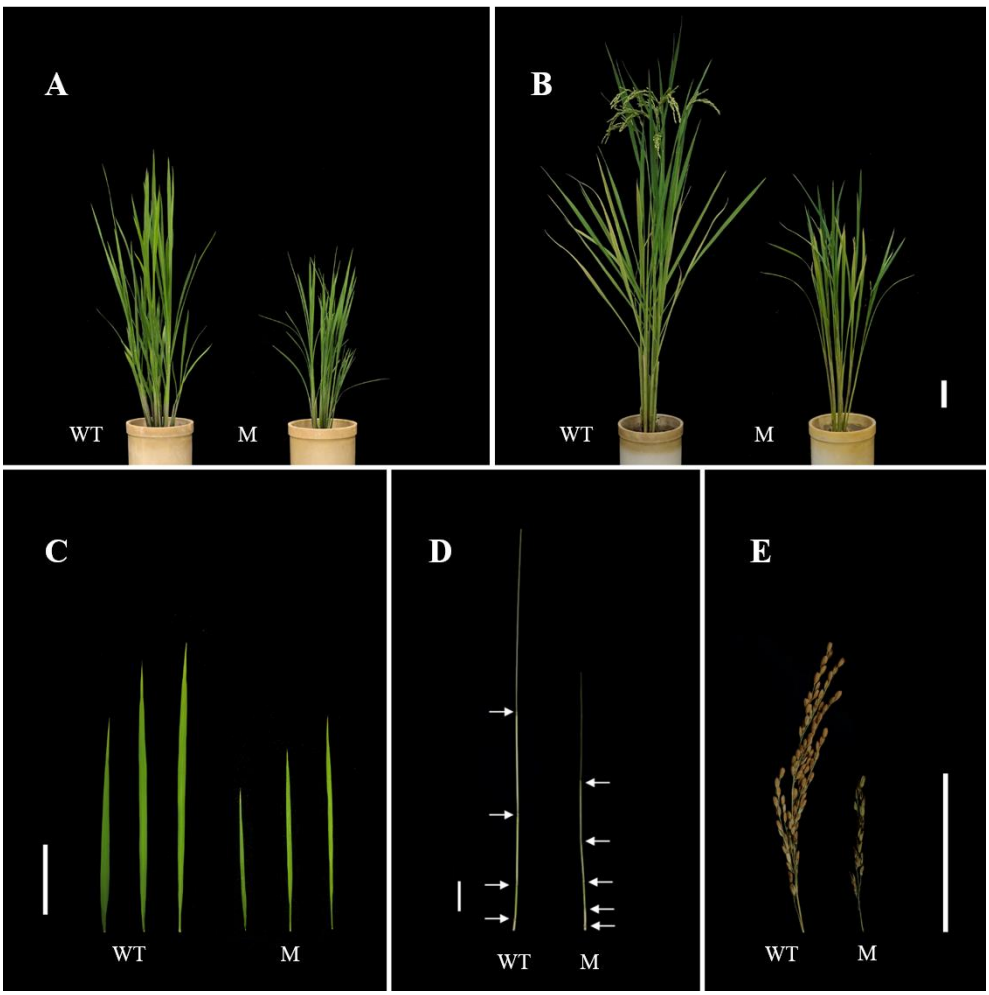


**Figure 1. Comparison of plant morphology between wild type and mutant.** WT, wild type; M, mutant. (A) Plant architecture in the late vegetative stage. (B) Plant architecture in ripening stage. (C) phenotype of leaves (left to right: flag leaf, second leaf, third leaf). (D) phenotype of Internode (white arrows indicate internode). (E) phenotype of panicle. Bar= 10cm

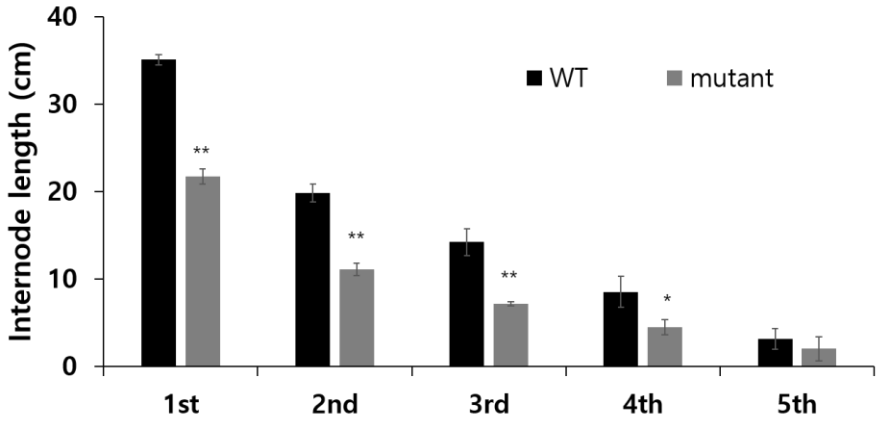


**Figure 2. Comparison of internode length between wild type and mutant.** The rate of decrease in mutant is significant from the upper four internodes. Values are the mean±s.d (n=10). Asterisks indicate the statistical significance levels according to an unpaired *t*-test: **, $p<0.01$ and *, $p<0.05$.

The second distinct morphological trait of the stunted growth mutant is the narrow leaf. Narrow leaves of mutant were clearly distinguished from four-leaf stage to mature plants. In the seedling stage, both dwarfism and narrow leaf appeared in mutant, but difference of leaf phenotype between wild type and mutant was more apparent than that of plant height. We compared the leaf width and length of the mutant and wild type. The width and length of flag leaves of the mutant were reduced by 46% and 34% compared to those of wild type, respectively (Figure. 3), while the width and length of second leaves from the top were reduced by 44% and 35% compared to those of the wild type, respectively (Figure. 4). According to the result, the degree of

decrease is higher in leaf blade width than length. Consequently, the ratio of the leaf blade length to the width significantly increased in mutant.

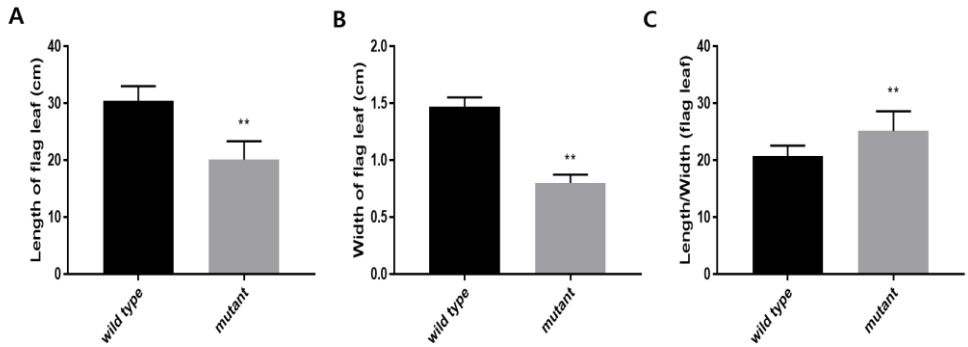


**Figure 3. Phenotypic comparison of flag leaves in wild type and mutant.** (A-B) Both of the length and width of flag leaf decreased in mutant compared to wild-type. (C) Length/width ratio indicates that width of leaves is more decreased than length of leaves. Values are the mean±s.d (n=10). Asterisks indicate the statistical significance levels according to an unpaired *t*-test: **, $p<0.01$ and *, $p<0.05$.

To explore the cause of the reduced leaf width, the anatomical analysis of the midpoint of second leaves from the top was performed at the heading stage. Longitudinal section was performed to compare cell shape and size between mutant and wild type. We observed the flanking stomatal row long cells (LC2s) in epidermis, which is the outer layer of cells covering all plant organs, on the abaxial side of leaf blade (Figure. 4). There was no significant change in leaf cell length and width between the mutant and wild type, whereas leaf blade showed significant decrease in both length and width in the mutant. This result suggested that mutant phenotype is due to the reduced cell proliferation.

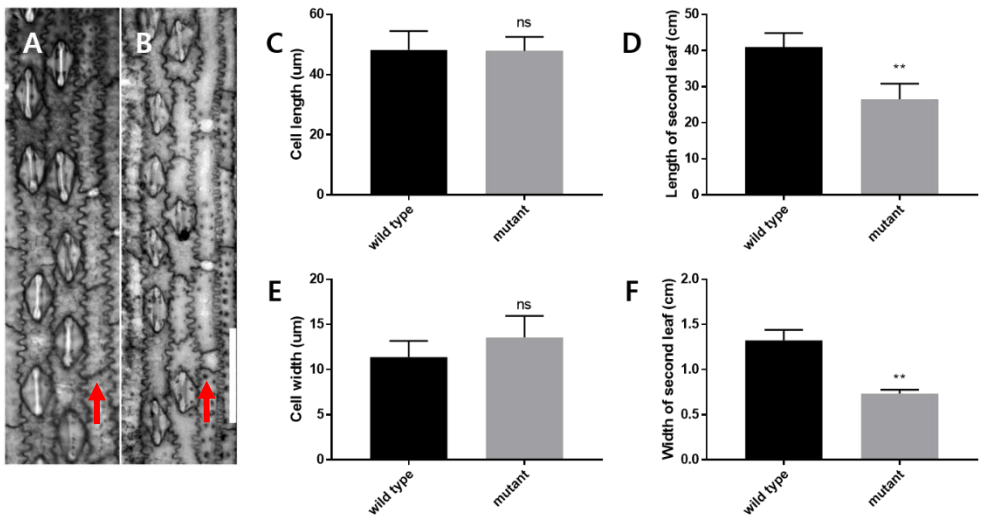


**Figure 4. Phenotypic analysis of mutant leaves at the heading stage.** (A, B) Epidermis of abaxial side of second leaf blade in wild type and mutant. Red arrow present flanking stomatal long cells (LC2). Bar = 50um. (C) Comparison of LC2 length in second leaf blade. (D) Comparison of length of second leaf blade. (E) Comparison of LC2 width in second leaf blade. (F) Comparison of width of second leaf blade. Values are the mean±s.d, n=6 (A, B, C, E), n=10 (D, F). Asterisks indicate the statistical significance levels according to an unpaired *t*-test: **, $p<0.01$ and *, $p<0.05$. NS, not significant.

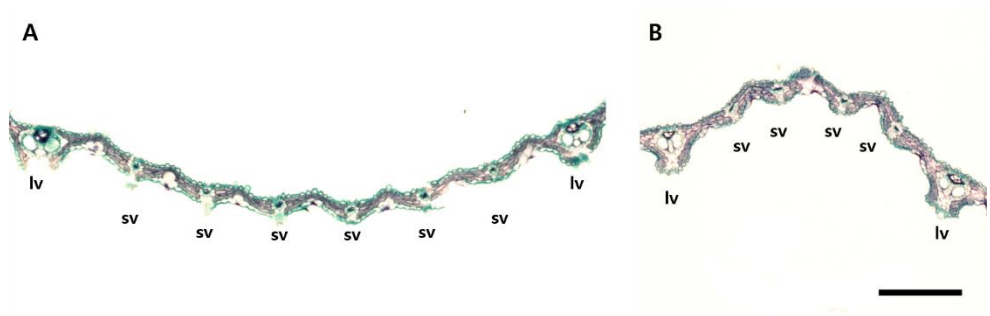


**Figure 5. Transverse section of leaf at the heading stage.** Region between two large veins in transverse section through the middle of second leave at the heading stage. The number of small vein is decreased in mutant (B) compared to wild type (A). lv, large vein; sv, small vein. Bar = 200um

In transverse section, we found that the number of both large and small vascular bundles were reduced in the mutant leaf blades (Figure. 5). The number of small vascular bundles between two large vascular bundles and the total number of vascular bundles on one side of mid-vein were reduced in the mutant (data not shown). These results indicated that the reduced number of vascular bundles contributes to the narrow leaf phenotype.

The third morphological trait is complete spikelet sterility. In addition to the spikelet sterility, the mutant displayed a delay of 20 to 25days in heading date (Table 2) and reduced panicle exertion (Figure. 8). Panicle number and length reduced by 35% and 57% respectively compared to those of wild type (Table 2).

Both spikelet of wild type and mutant consisted of a flower with one pistil, six stamens, and two lodicules subtended by palea and lemma. However, mutant spikelet presented slightly thin and flattened external shape due to the narrower lemma and palea compared to the wild type. Besides, the mutant spikelet showed small gap between the upper part of lemma and palea (Figure. 6-E, F). Anthers of mutant were smaller and more pale compared to that of wild type (Figure 6-I, K). Pollens grains of mutant exhibited unviable as revealed by iodine potassium iodide ($I_2$-KI) staining. Many mutant pollen grains were small and defective. In contrast to the wild type, less than 30% of the mutant pollen grains showed relatively normal

morphology (Figure. 6-J, L). Wild type anthers dehisced and mature pollen grains were normally released for pollination, while mutant failed in both anthesis and anther dehiscence partially. Ripened grains of mutant were investigated to count filled or unfilled grains. All of the mutant grains were unfilled. Some of them were abnormally developed as shown in Figure. 7-D. Others were even not pollinated.

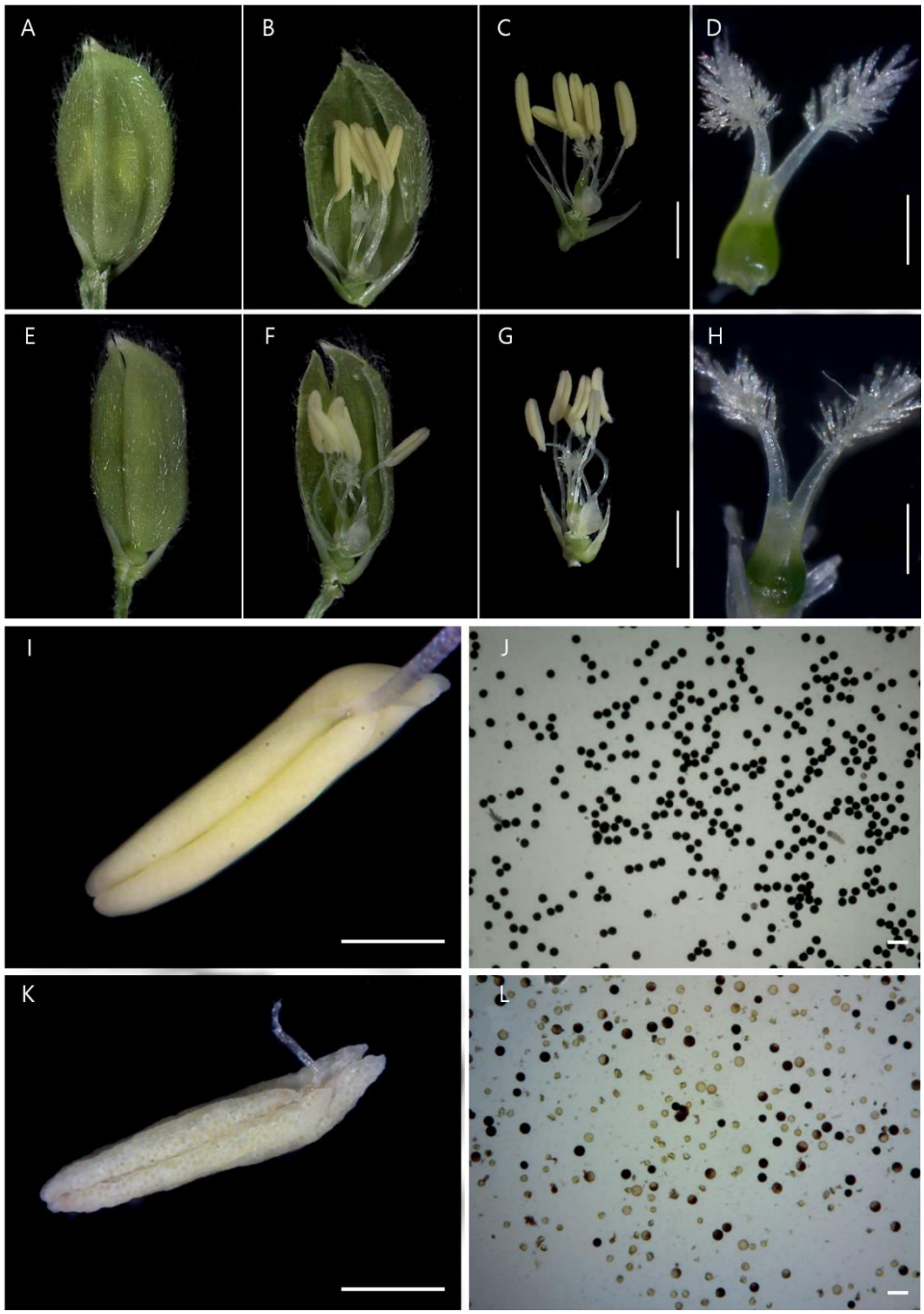


**Figure 6. Comparison of spikelet organs and pollen viability between wild type and mutant.** Wild type (A-D, I-J). Mutant (E-H, K-L). A to C, Spikelet of wild type. Bar = 1mm. D, Pistil of wild type. Bar = 500um. E to G, Spikelet of mutant. Bar = 1mm. H, Pistil of mutant. Bar = 500um. Anther of wild type (I) and mutant (K). Bar = 500um. Mature pollen grains stained with $I_2$-KI solution in wild type (J) and mutant (L) Bar = 100um.

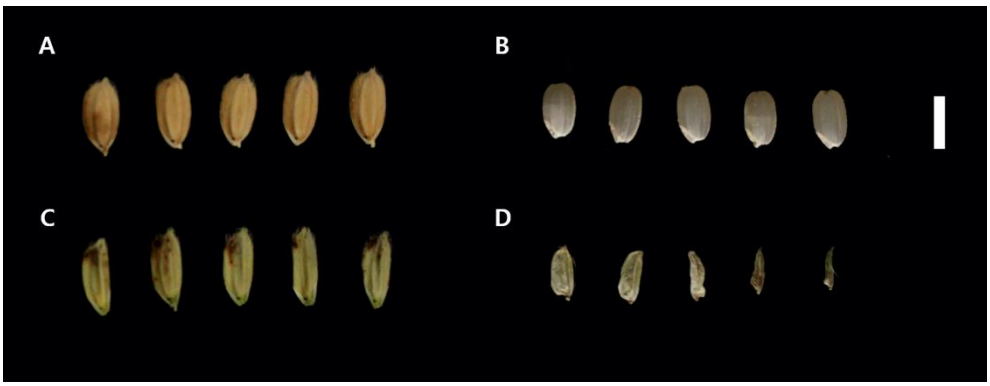


**Figure 7. Representative seeds in wild type and abnormally developed grains in mutant.** Wild type (A-B), Mutant (C-D). Bar = 0.5cm. Mutant showed complete sterility.

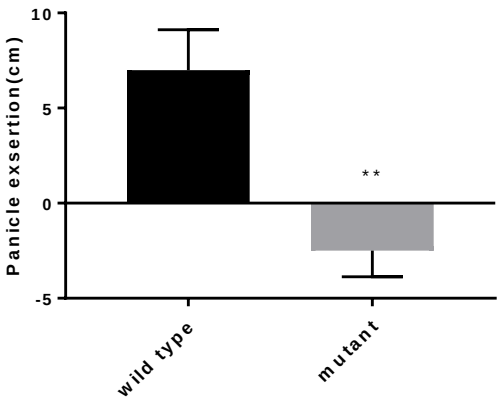


**Figure 8. Comparison of panicle exsertion between wild type and mutant.** Values are the mean±s.d, n=10. Asterisks indicate the statistical significance levels according to an unpaired *t*-test: **, $p<0.01$ and *, $p<0.05$. NS, not significant.

**Table 2. Comparison of agronomic traits between wild type and mutant plants**

| | DTH | PH (cm)** | CL (cm)** | PL (cm)** | PN (No.)** |
|---|---|---|---|---|---|
| **wild type** | 110 | 108.3±4.88 | 84.85±4.25 | 19.28±1.42 | 8.9±2.18 |
| **mutant** | 135 | 71.49±4.62 | 48.89±1.98 | 8.33±1.36 | 5.8±1.75 |

Values are the mean±s.d (n=10). An unpaired *t*-test was used to generate the *p* value. *, $p<0.05$. **, $p<0.01$. NS, not significant. DTH, days to heading; PH, plant height; CL, culm length; PL, plant length; PN, panicle number.

## Genetic analysis of the mutant gene

The individual plants of $F_1$ and $F_2$ progenies from cross of mutant to its parent cultivar Samgwang were used to investigate whether the mutant is controlled by a single gene. The phenotype of $F_1$ progenies exhibited wild type architecture, suggesting that the mutant trait was recessive. In $F_2$ population, segregation of wild type and mutant type was a good fit to the 3:1 segregation ratio ($\chi 2$=0.906, P=0.341, $\chi 2_{0.05(1)}$=3.841). The result indicated that the mutant trait is controlled by a single recessive nuclear gene (Table 3).

**Table 3. Segregation ratio of $F_2$ population**

| Cross combination | Generation | n | Ratio tested | No. of plants | | Total | Chi-square ($\chi 2$) | *P* |
|---|---|---|---|---|---|---|---|---|
| | | | | Wild type | Mutant | | | |
| Mutant /Samgwang | F2 | 178 | 3:1 | 139 | 39 | 178 | 0.906 | 0.341 |

## Genetic mapping of the mutant gene

To determine the chromosomal location of the mutant related gene, bulked segregant analysis (BSA) of $F_2$ plants from the cross between mutant and Milyang23 was performed using 109 STS markers distributed on the 12 chromosomes. As a result, a candidate region was located between the STS markers S05000 and S05032 on the short arm of chromosome 5 (Figure. 9).

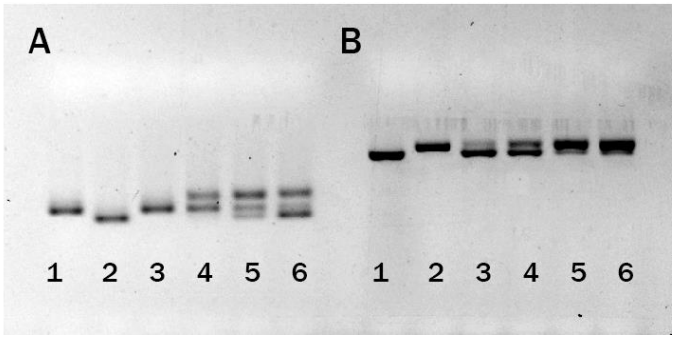


**Figure 9. Bulked segregant analysis result.** (A) S05000 marker. (B) S05032 marker. 1, mutant; 2, Milyang23; 3-4, mutant type bulks; 5-6, wild type bulks.

To fine map the flanking region, InDel markers, CAPS and dCAPS markers within the flanking markers were designed based on the sequence polymorphism between *Indica* and *Japonica* rice varieties (Table 1). Using 840 plants (96 $F_2$, 544 $F_3$, 200 $F_4$ plants), the mutant locus was delimited to an approximately 84kb physical distance, flanked by markers NC0501.48 and NdC0501.56 (Figure. 10). Data obtained from fine mapping and available MSU annotation database (http://rice.plantbiology.msu.edu/) indicated that twelve candidate genes were located in this 84kb genomic region (Table 4).

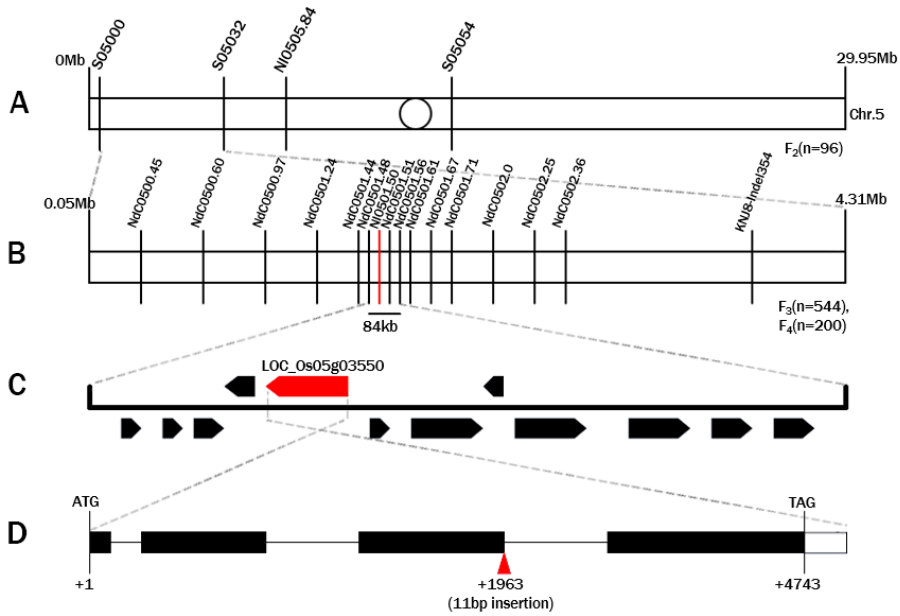


**Figure 10. Map-based cloning of the mutant.** (A) Schematic diagram of mapping of mutant locus with BSA. (B) Fine mapping of the mutant locus. (C) Twelve candidate genes in the flanking region identified by fine mapping. (D) The candidate gene construction and splicing pattern; the 11bp insertion is identified in the third exon of *LOC_Os05g03550*. Exon, black box; intron, black line; UTR, white solid box; ATG, initiation codon; TAG, termination codon.

**Table4. Predicted genes in the mapping region**

| Gene name | Predicted function |
|---|---|
| *LOC_Os05g03510* | Putative uncharacterized protein |
| *LOC_Os05g03520* | Putative uncharacterized protein |
| *LOC_Os05g03530* | Tetraspanin family protein, putative, expressed |
| *LOC_Os05g03540* | Putative uncharacterized protein |
| *LOC_Os05g03550* | MYB family transcription factor, putative, expressed |
| *LOC_Os05g03560* | Putative uncharacterized protein |
| *LOC_Os05g03574* | Putative uncharacterized protein |
| *LOC_Os05g03590* | Putative uncharacterized protein |
| *LOC_Os05g03600* | Retrotransposon protein, putative, unclassified, expressed |
| *LOC_Os05g03610* | Phospholipase C, putative, expressed |
| *LOC_Os05g03620* | TKL_IRAK_CR4L.4 - the CR4L subfamily has homology with Crinkly4, expressed |
| *LOC_Os05g03630* | DnaJ domain containing protein, expressed |

Rice Genome Annotation Project database (http://rice.plantbiology.msu.edu)

**Sequence analysis of the candidate gene**

To determine the casual mutation, genomic DNA of the flanking region was sequenced. Whole genome sequencing of mutant was conducted using Illumina HiSeq 2500 and the result was aligned to Nipponbare 'reference sequence' to detect the causal mutation point. According to the sequencing result, only one variant, 11bp insertion at physical position of 1,505,063 bp on chromosome 5, was detected in the flanking region. The 11bp insertion was occurred in the genic region of *LOC_Os05g03550* and no other variants were detected in any other candidate genes.

To verify the insertion, InDel marker located outside the potential insertion region was designed and used to screen the $F_2$ population from crosses of mutant to Samgwang and Milyang23. Co-segregation test showed all genotypes co-segregated with the matching phenotypes (Figure. 11-A). To investigate whether the insertion was present as a natural variant in other cultivars, 32 typical *indica* and *japonica* rice cultivars (6 *aus*, 5 *tropical-japonica*, 5 *temperate japonica*, 5 *aromatic*, 7 *indica*, and 4 *tongil* types) were genotyped with the InDel marker that detect the insertion. The result showed that all 32 varieties carries the wild type allele (Figure. 11-B).

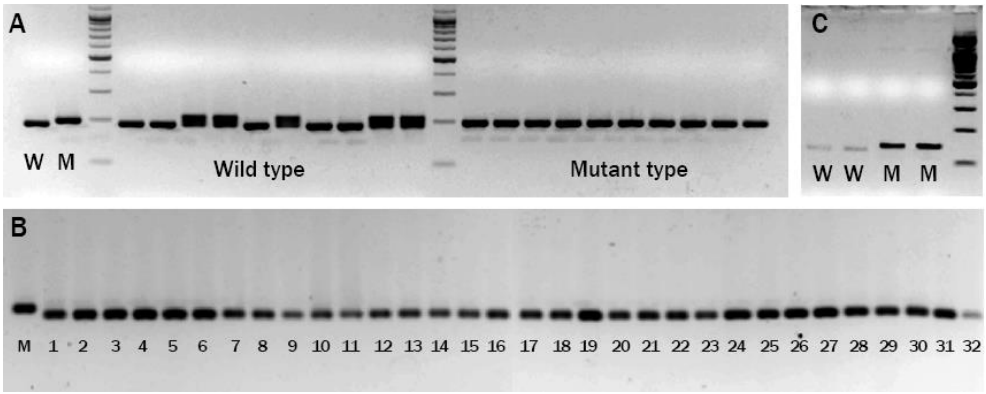


**Figure 11. Co-segregation test.** (A) Co-segregation test on $F_2$ individuals generated between mutant and Samgwang. W, wild (188bp); M, mutant (199bp) (B) Co-segregation test on other varieties. M, mutant; 1, ARC10177; 2, Kalamkati; 3, N22; 4, Jasmine85; 5, Dular; 6, Kasalath; 7, Della; 8, Azucena; 9, Lemont; 10, Moroberekan; 11, Cp-slo; 12, Norin20; 13, Chuchung; 14, Nipponbare; 15, Hwachung; 16, Koshihikari; 17, Bico Branco; 18, Firooz; 19, Nova; 20, N12; 21, Sadri Belyi; 22, 93-11; 23, IR64; 24, TN1; 25, Tetep; 26, IR36; 27, Pokkali; 28, Minghui63; 29, Samgang; 30, Tongil; 31, Milyang23; 32, Dasan. (C) semi-quantitative RT-PCR analysis of fragment including mutant locus in wild type and mutant to confirm the insertion in cDNA. W, wild (128bp); M, mutant (139bp).

Comparison of sequence between Samgwang and mutant revealed that 11bp insertion was occurred at the third exon of *LOC_Os05g03550* and introduced a premature stop codon at the 664th residue of *LOC_Os05g03550* (Figure. 12), which is located in front of conserved domains of the gene, first SANT domain (SANT1) at the 724th residue and second SANT domain (SANT2) at the 933th residue. Based on MSU gene prediction, *LOC_Os05g03550* encodes a protein of 1,581 amino acid and expected to have a putative MYB family transcription factor activity (http://rice.plantbiology.msu.edu), whereas IRGSP predicted differently. Using semi RT-PCR, we found gene form corresponds to MSU's prediction.

Therefore, this finding suggests that premature stop codon caused by 11bp insertion could result in malfunction of the LOC_Os05g03550.


**Figure 12. Sequence analysis between wild type and mutant.** (A) Comparison of nucleotide sequence in the insertion position in cDNA. (B) Comparison of amino-acid sequence in the mutation point.

**Sequence homology analysis of LOC_Os05g03550**

Coding sequence of *LOC_Os05g03550* consisted of 4,743 nucleotides over 4 exons, and encoded a putative 1,581-amino acid protein. The distinct feature of the predicted protein is a pair of SANT (SWI3/ADA2/N-CoR/TFIII-B) domains. The paired SANT domains (SANT1 and SANT2) are encoded in the forth and the largest exon of the gene. A BLAST search for proteins in rice and other organisms identified orthologs in other plant species, such as *Oryza brachyantha* (XP_006654948.2), *Brachypodium distachyon* (XP_010231802.1), *Sorghum bicolor* (XP_021303528.1), and *Zea mays* (NP_001349284.1) with 58-83% amino acid identity, but no homologs in rice. Furthermore, characterization of those predicted proteins has not been verified yet. However, regarding to a BLAST search for domain sequences, the conserved two SANT domains revealed that high sequence similarity with those of the animal HDAC subunits SMRT and N-CoR, around 60% of similarity and 40% of identify. Also PWR in Arabidopsis (NP_190793.2), whose function has been demonstrated to be involved in histone deacetylation, has 62% of identity and 78% of similarity with the SANT domains in LOC_Os05g03550 (Figure. 13).

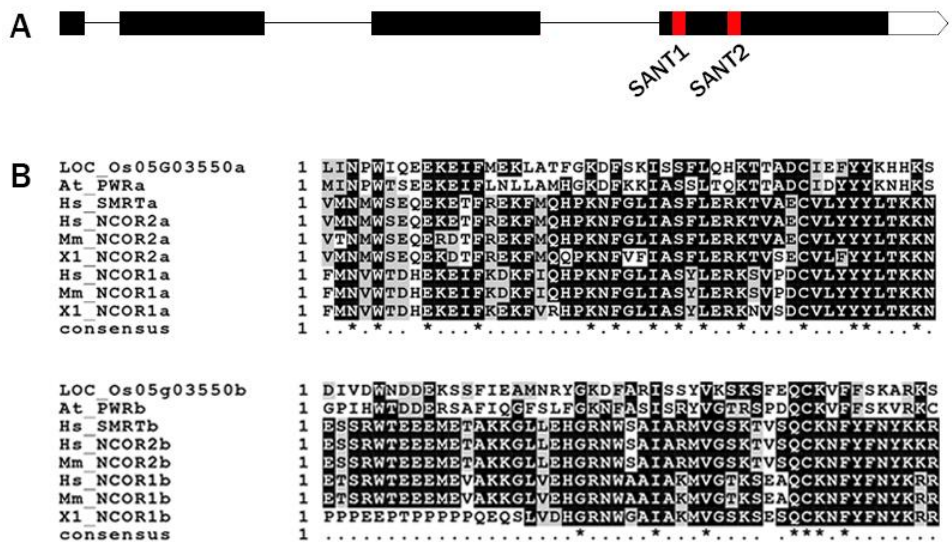


**Figure 13. Multiple sequence alignment of SANT domain of LOC_Os05g03550.** (A) A schematic gene diagram of *LOC_Os05g03550* showing SANT domain regions in close proximity within the forth exon. (B) Sequence homology analysis of the two SANT domains in LOC_Os05g03550 and those from plant and animal homologs (Kim et al., 2016). Identical amino acids are highlighted in black and similar amino acids are highlighted in gray. Asterisk indicates the identical amino acids. a, SANT1 domain; b, SANT2 domain; At, *Arabidopsis thaliana*; Hs, *Homo sapiens*; Mm, *Mus musculus*; Xl, *Xenopus laevis.*

**Expression analysis of *LOC_Os05g03550***

To investigate the expression pattern of *LOC_Os05g03550*, quantitative Real time PCR (qRT-PCR) was conducted with total RNA from several organs at different stages.

First, qRT-PCR was performed with leaves of wild type at three different stages, including seedling, vegetative and reproductive stage. qRT-PCR analysis detected the expression of the gene in all three stages. In addition, the expression level was gradually increased and achieved its maximal level at the reproductive stage (Figure. 14-A). Expression analysis of three different organs in wild type, including flag leaf, internode and young panicle, at the reproductive stage indicated that the gene was more highly expressed in flag leaf relative to internode and panicle (Figure. 14-B). These findings indicate that constantly increasing expression level of the gene is matched to morphological impact in mutant which shows a more severe defect at the reproductive stage.

To examine whether the difference of expression level appears in mutant, we performed qRT-PCR of flag leaf in wild type and mutant. Interestingly, the result presented that the relative expression level of mutant was significantly higher than that of wild type (Figure. 14-C). The cause of the expression level change in mutant remains unclear, but it may be considered that abnormal protein in mutant could not fulfil a required function, and induce a transcription signal continuously for complementation.

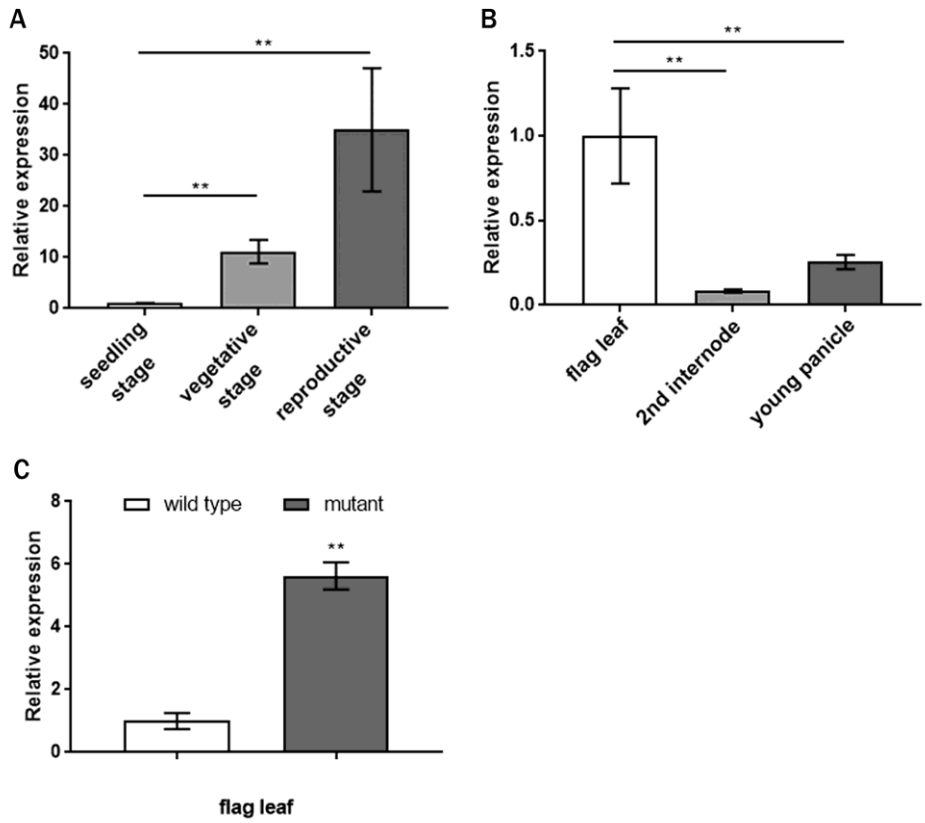


**Figure 14. qRT-PCR analysis of *LOC_Os05g03550*.** (A) Expression level of the gene in wild type at different developmental stages. (B) Expression level of the gene in wild type at different organs. (C) Comparison of expression level of the gene in flag leaf between wild type and mutant. Asterisks indicate the statistical significance levels according to an unpaired *t*-test: **, $p<0.01$ and *, $p<0.05$. NS, not significant.

# DISCUSSION

In this study, we found a stunted growth mutant in rice treated with chemical mutagenesis. Fine mapping showed that the candidate gene of mutant was located in an interval of 84kb between NC0501.48 and NdC0501.56 markers, which is on the short arm of chromosome 5 (Figure. 10). As a result of sequence analysis, 11 nucleotides insertion was found in *LOC_Os05g03550*, which contains two conserved SANT domains. The mutant exhibited overall retardation of plant development during whole growth period. Mutant seedlings developed small plant height and narrow leaf compared with wild type seedlings at the vegetative stage, while at the reproductive stage, mutant plants showed late flowering, spikelet sterility, and short panicle.

A detailed analysis in leaves has revealed that the reduced stature of stunted growth mutant results from a cell proliferation defect. During plant development, final organ size is reliant upon growth rate and duration. At the cellular level, growth rate is resulted by reciprocal action between cell proliferation and expansion. In the proliferative phase, cell number increases rapidly, whereas cell size remains relatively constant. When cell division rate decreases, cell expansion appears, followed by increase of organ size. By varying the length and pace of mitotic activity, the total number of cells

and organ size is altered (Beemster et al., 2006; Donnelly et al., 1999; Lee et al., 2012). The leaf is a representative organ to examine the regulating mechanisms of organ size owing to its determinate growth (Andriankaja et al., 2012; Donnelly et al., 1999; Ichihashi et al., 2011). In the stunted growth mutant, an anatomical analysis revealed that no significant difference in cell size, whereas leaf size showed significantly reduction compared with wild type. This means cell proliferation is not properly working in the mutant. In addition, significant decrease in the total number of vascular bundles was also examined, which means a reduced cell number in the lateral direction. This result is similar with other narrow leaf mutants whose phenotype mainly resulted from a defect in cell proliferation and a reduced vascular bundles, including *nal1*, *nal7* and *tdd1* (Li et al., 2009). This result suggests that *LOC_Os05g03550* plays a role in the control of cell proliferation to maintain normal plant stature. Besides, several narrow leaf mutants, *nal7* and *tdd1*, with reduced vascular bundles were also found to be associated with abnormal auxin biosynthesis or transport (Fujino et al., 2008; Sazuka et al., 2009). Therefore, further studies about linkage to auxin will be helpful to understand function of *LOC_Os05g03550*.

Spikelet sterility in the stunted growth mutant has been identified that it is mainly caused by a defect in pollen grains through pollen viability test, although the partial failure of anthesis and anther indehiscence was also

detected. At first, environmental effect, such as low temperature, during ripening stage of the mutant, which was delayed due to the late flowering, was also considered, but mutants grown in green house under the temperature control showed the same level of sterility with those grown in paddy field.

In rice, it has been identified that deposition of starch metabolites in the pollen grain is critical for its viability (Raghavan, 1988). Significant mechanical force of pollen grains which swell rapidly ruptures the enzymatically weakened septum for the release (Matsui et al., 1999). In the stunted growth mutant, it was observed that a few anthers did dehisce but seed-setting of them was failed. This indicates that anther indehiscence is influential, but not absolutely essential reason for the spikelet sterility of the mutant. Among male sterile mutants in previous studies, the *anther indehiscence1* (*aid1)* mutant showed partial to complete spikelet sterility based on defect in the viability of pollen grains and the extent of anther dehiscence. Type1 spikelet of *aid1* were sterile due to a starch accumulation defect in pollen grains, while type2 spikelet of *aid1* appeared anther dehiscence failure regarding to septum degradation (Zhu et al., 2004). In anther study, the *defective pollen wall 2* (*dpw2*) indicated complete male sterility due to increased cutin level in anther and decreased amounts of lipidic and phenolic compounds in pollen wall, which make aborted pollen grains and anther dehiscence failure (Xu et al., 2017).

Taken together, the exact reason for various levels of fertility defects in the stunted growth mutant is not clear yet, but it is suggested that lack of starch accumulation of pollen grains led to low viability based on the result of $I_2$-KI staining. Insufficient pressure of the non-swollen pollen grains might result in partial anther indehiscence in the mutant. However, further experiments for degradation of tapetum, or deposition of starch metabolites in pollen developmental stages are necessary.

In addition to pollen sterility, the stunted growth mutant exhibited unclosed spikelet. A gap resulted from incomplete matching between lemma and palea is similar with *OPEN BEAK (OPB)* mutants. In mutants of *OPB*, lemma and palea were suppressed in their lateral growth, thus had open beak-like lemma/palea phenotype which is unable to enclose internal floral organs and have a curved tip of the lemma toward the palea. The *OPB* is regarded to have function in cell proliferation based on the abnormal cell division pattern and ectopic expression of some *KNOX* genes (Horigome et al., 2009; Yoshida and Nagato, 2011). Further careful analysis is necessary to reveal a role of *LOC_Os05g03550* in lemma and palea development.

According to the genetic analysis, it was verified that the stunted growth mutant is controlled by a single recessive gene. However, the mutant showed wide range of developmental defects. This finding suggested that a single gene may be involved in diverse biological process like a

transcription factor. Through genetic mapping, we fine-mapped a candidate gene, *LOC_Os05g03550*, containing two SANT domains. Many previous studies revealed that SANT domain-containing proteins interact with a number of regulatory proteins, forming complexes that function in the control of the expression of target genes. Accordingly, small deletions in SANT domains introduce transcriptional defects that are consistent with the complete deletion of the target genes (Barbaric et al., 2003; Boyer et al., 2002; Sterner et al., 2002). The presence of two SANT domains in LOC_Os05g03550 and the spacing between them (165 amino acids) are similar to the domain structures of HDAC subunits silencing mediator for retinoic acid and thyroid receptor (SMRT) and nuclear receptor co-repressor (N-CoR) whose first and second SANT domains are necessary for HDAC activation and binding to unacetylated histone tails, respectively (Guenther et al., 2001; Yu et al., 2003).

SANT domains in LOC_Os05g03550 are speculated as a subunit of histone modification complex. SANT domain is known as MYB-related domain, which is mainly found in proteins involved in chromatin-remodeling complexes. Although SANT domains show high sequence similarity to the DNA-binding domain (DBD) of Myb-related proteins, it is proved to function as histone binding, not DNA binding (Boyer et al., 2004). SANT domain represents relatively acidic isoelectric point (pI<7) and a

negative electrostatic surface indicating a histone binding ability in contrast with highly electropositive surface potential (pI= ~10) of Myb DBD that is consistent with DNA binding (Boyer et al., 2004). In terms of histone binding feature, pI of LOC_Os05g03550 was measured as 6.3, which reflected a potential histone modification function of the gene.

Multiple alignment of SANT domain sequences with N-CoR and SMRT showed high similarity around 60% (Figure.13). A lot of studies in animal and yeast demonstrated the association of SANT domain-containing enzyme subunits in chromatin remodeling activity, including histone acetylation, histone deacetylation, and ATP-dependent chromatin remodeling (Boyer et al., 2004). Especially, an ortholog in Arabidopsis, a SANT domain-containing protein POWERDRESS (PWR) with 78% similarity in domain sequence, was recently reported. In PWR, mutant exhibited pleotropic defects similar in morphological trait with *LOC_Os05g03550* mutant, such as abnormal shape of carpels and siliques, small plant size, disrupted flowering time and aberrant petal shape (Yumul et al., 2013), which are related to floral stem cell termination. In addition, Suzuki et al. (2018) suggested that PWR plays a combinatorial role in establishing a complex with HOS15 and HDA9, which functions in cell proliferation rate in leaf primordia. The complex also controls the progression from the juvenile to adult phase of leaf trait. Furthermore, Chen et al. (2016) studied a histone

deacetylase called HDA9 in Arabidopsis and demonstrated a novel role of HDA9 which acts in complex with PWR and transcription factor WRKY53 in promoting senescence. PWR instructs HDA9 to remove acetyl groups from the histones of aging-associated genes in order to switch these genes off.

As corepressors function properly when they combine with HDAC for complex, we expected mutants which lose histone deacetylation function will show similar phenotype with the stunted growth mutant. Therefore, we searched loss-of-function studies of rice HDAC genes to compare each phenotype. Hu et al. (2009) experimented down-regulation of rice HDAC genes affects in various developmental aspects. For example, down regulation of *HDA703* by amiRNA reduced rice peduncle elongation, followed by partially wrapped panicles and obtained various level of sterility. Inactivation of a closely related homolog *HDA710* by RNAi affected reduced vegetative growth influenced by poorly developed roots. In Arabidpsis, *AtHD1/HDA19* loss-of-function mutant showed diverse abnormalities including seedling development, plant height, floral organ number and morphology, reduced fertility and fruit morphology (Benhamed et al., 2006; Tian and Chen, 2001; Tian et al., 2005; Zhou et al., 2005). In addition, *HDA704* RANi displayed dwarf in plant height and twisted flag leaf morphology. Down-regulation of *HDT702* produced narrowed leaves

and stems. These data suggest that rice HDAC genes may have divergent developmental functions (Hu et al., 2009). Consequently, these findings show mutations in HDAC genes appear similar developmental defects with those of the stunted growth mutant, and support correlation of LOC_Os05g03550 with HDAC function.

Taken together, LOC_Os05g03550 mutant phenotype exhibited analogy with PWR in Arabidopsis in terms of potential chromatin remodeling factor. Therefore, it could be an important evidence to support the hypothesis that LOC_Os05g03550 might have a transcriptional regulation role by forming a transcriptional repression complex with histone deacetylase and other regulatory factors. In other words, it is possible that the malfunction of LOC_Os05g03550 in mutant yields pleiotropic defects in developmental events by repressing related gene expression involving in numerous biological processes such as cell proliferation, floral transition, or starch accumulation.

In conclusion, the new stunted growth gene identified in this study not only diversifies rice mutation germplasm, but also provides a good starting point for elucidating the details of plant growth mechanisms associated with a new SANT domain-containing protein in rice.

# REFERENCE


Aasland, R., Francis Stewart, A., and Gibson, T. (1996). The SANT domain: a putative DNA-binding domain in the SWI-SNF and ADA complexes, the transcriptional corepressor N-CoR and TFIIIB. Trends in Biochemical Sciences *21*, 87–88.

Andriankaja, M., Dhondt, S., De Bodt, S., Vanhaeren, H., Coppens, F., De Milde, L., Mühlenbock, P., Skirycz, A., Gonzalez, N., Beemster, G.T.S., et al. (2012). Exit from proliferation during leaf development in Arabidopsis thaliana: a not-so-gradual process. Dev. Cell *22*, 64–78.

Banerjee, J., and Maiti, M.K. (2010). Functional role of rice germin-like protein1 in regulation of plant height and disease resistance. Biochem. Biophys. Res. Commun. *394*, 178–183.

Barbaric, S., Reinke, H., and Hörz, W. (2003). Multiple mechanistically distinct functions of SAGA at the PHO5 promoter. Mol. Cell. Biol. *23*, 3468–3476.

Beemster, G.T.S., Vercruysse, S., De Veylder, L., Kuiper, M., and Inzé, D. (2006). The Arabidopsis leaf as a model system for investigating the role of cell cycle regulation in organ growth. J. Plant Res. *119*, 43–50.

Benhamed, M., Bertrand, C., Servet, C., and Zhou, D.-X. (2006). Arabidopsis GCN5, HD1, and TAF1/HAF2 interact to regulate histone acetylation required for light-responsive gene expression. Plant Cell *18*, 2893–2903.

Boyer, L.A., Langer, M.R., Crowley, K.A., Tan, S., Denu, J.M., and Peterson, C.L. (2002). Essential role for the SANT domain in the functioning of multiple chromatin remodeling enzymes. Mol. Cell *10*, 935–942.

Boyer, L.A., Latek, R.R., and Peterson, C.L. (2004). The SANT domain: a unique histone-tail-binding module? Nature Reviews Molecular Cell Biology *5*, 158–163.

Busov, V.B., Brunner, A.M., and Strauss, S.H. (2008). Genes for control of plant stature and form. New Phytol. *177*, 589–607.

Chen, X., Lu, L., Mayer, K.S., Scalf, M., Qian, S., Lomax, A., Smith, L.M., and Zhong, X. (2016). POWERDRESS interacts with HISTONE DEACETYLASE 9 to promote aging in Arabidopsis. Elife *5*.

Chin, J.-H., Kim, J.-H., Jiang, W., Chu, S.-H., Woo, M.-O., Han, L., et al. (2007). Identification of subspecies-specific STS markers and their association with segregation distortion in rice (Oryza sativa L.). J Crop Sci Biotech *10*, 175–184.

David, C.C., Otsuka, K. 1994. Modern rice technology and income distribution in Asia.

Boulder, CO, USA: Lynne Reinner, 3–17.

Deng, Z.Y., Liu, L.T., Li, T., Yan, S., Kuang, B.J., Huang, S.J., Yan, C.J., and Wang, T. (2015). OsKinesin-13A is an active microtubule depolymerase involved in glume length regulation via affecting cell elongation. Sci Rep *5*, 9457.

Donald, C.M. (1968). The breeding of crop ideotypes. Euphytica *17*, 385–403.

Donnelly, P.M., Bonetta, D., Tsukaya, H., Dengler, R.E., and Dengler, N.G. (1999). Cell cycling and cell enlargement in developing leaves of Arabidopsis. Dev. Biol. *215*, 407–419.

Fujino, K., Matsuda, Y., Ozawa, K., Nishimura, T., Koshiba, T., Fraaije, M.W., and Sekiguchi, H. (2008). NARROW LEAF 7 controls leaf shape mediated by auxin in rice. Mol. Genet. Genomics *279*, 499–507.

Guenther, M.G., Barak, O., and Lazar, M.A. (2001). The SMRT and N-CoR corepressors are activating cofactors for histone deacetylase 3. Mol. Cell. Biol. *21*, 6091–6101.

Horigome, A., Nagasawa, N., Ikeda, K., Ito, M., Itoh, J.-I., and Nagato, Y. (2009). Rice open beak is a negative regulator of class 1 knox genes and a positive regulator of class B floral homeotic gene. Plant J. *58*, 724–736.

Hu, J., Zhu, L., Zeng, D., Gao, Z., Guo, L., Fang, Y., Zhang, G., Dong, G., Yan, M., Liu, J., et al. (2010). Identification and characterization of NARROW AND ROLLED LEAF 1, a novel gene regulating leaf morphology and plant architecture in rice. Plant Mol. Biol. *73*, 283–292.

Hu, Y., Qin, F., Huang, L., Sun, Q., Li, C., Zhao, Y., and Zhou, D.-X. (2009). Rice histone deacetylase genes display specific expression patterns and developmental functions. Biochemical and Biophysical Research Communications *388*, 266–271.

Ichihashi, Y., Kawade, K., Usami, T., Horiguchi, G., Takahashi, T., and Tsukaya, H. (2011). Key proliferative activity in the junction between the leaf blade and leaf petiole of Arabidopsis. Plant Physiol. *157*, 1151–1162.

Itoh, J.-I., Nonomura, K.-I., Ikeda, K., Yamaki, S., Inukai, Y., Yamagishi, H., Kitano, H., and Nagato, Y. (2005). Rice Plant Development: from Zygote to Spikelet. Plant Cell Physiol *46*, 23–47.

Kim, Y.J., Wang, R., Gao, L., Li, D., Xu, C., Mang, H., Jeon, J., Chen, X., Zhong, X., Kwak, J.M., et al. (2016). POWERDRESS and HDA9 interact and promote histone H3 deacetylation at specific genomic sites in Arabidopsis. PNAS *113*, 14858–14863.

Lee, L.Y.C., Hou, X., Fang, L., Fan, S., Kumar, P.P., and Yu, H. (2012). STUNTED mediates the control of cell proliferation by GA in Arabidopsis. Development *139*, 1568–1576.

Li, M., Xiong, G., Li, R., Cui, J., Tang, D., Zhang, B., Pauly, M., Cheng, Z., and Zhou, Y. (2009). Rice cellulose synthase-like D4 is essential for normal cell-wall biosynthesis and plant growth. Plant J. *60*, 1055–1069.

Li, W., Wu, C., Hu, G., Xing, L., Qian, W., Si, H., Sun, Z., Wang, X., Fu, Y., and Liu, W. Characterization and Fine Mapping of a Novel Rice Narrow Leaf Mutant nal9. Journal of Integrative Plant Biology *55*, 1016–1025.

Matsui, T., Omasa, K., and Horie, T. (1999). Mechanism of Anther Dehiscence in Rice ( Oryza sativa L.). Ann Bot *84*, 501–506.

Michelmore, R.W., Paran, I., and Kesseli, R.V. (1991). Identification of markers linked to disease-resistance genes by bulked segregant analysis: a rapid method to detect markers in specific genomic regions by using segregating populations. Proc. Natl. Acad. Sci. U.S.A. *88*, 9828–9832.

Qi, J., Qian, Q., Bu, Q., Li, S., Chen, Q., Sun, J., Liang, W., Zhou, Y., Chu, C., Li, X., et al. (2008). Mutation of the rice Narrow leaf1 gene, which encodes a novel protein, affects vein patterning and polar auxin transport. Plant Physiol. *147*, 1947–1959.

Raghavan, V. (1988). Anther and Pollen Development in Rice (oryza Sativa). American Journal of Botany *75*, 183–196.

Sato, Y., Sentoku, N., Miura, Y., Hirochika, H., Kitano, H., and Matsuoka, M. (1999). Loss-of-function mutations in the rice homeobox gene OSH15 affect the architecture of internodes resulting in dwarf plants. EMBO J. *18*, 992–1002.

Sazuka, T., Kamiya, N., Nishimura, T., Ohmae, K., Sato, Y., Imamura, K., Nagato, Y., Koshiba, T., Nagamura, Y., Ashikari, M., et al. (2009). A rice tryptophan deficient dwarf mutant, tdd1, contains a reduced level of indole acetic acid and develops abnormal flowers and organless embryos. Plant J. *60*, 227–241.

Sterner, D.E., Wang, X., Bloom, M.H., Simon, G.M., and Berger, S.L. (2002). The SANT domain of Ada2 is required for normal acetylation of histones by the yeast SAGA complex. J. Biol. Chem. *277*, 8178–8186.

Struhl, K. (1998). Histone acetylation and transcriptional regulatory mechanisms. Genes Dev. *12*, 599–606.

Suzuki, M., Shinozuka, N., Hirakata, T., Nakata, M.T., Demura, T., Tsukaya, H., and Horiguchi, G. (2018). OLIGOCELLULA1/HIGH EXPRESSION OF OSMOTICALLY RESPONSIVE GENES15 Promotes Cell Proliferation With HISTONE DEACETYLASE9 and POWERDRESS During Leaf Development in Arabidopsis thaliana. Front. Plant Sci. *9*:580.

Tian, L., and Chen, Z.J. (2001). Blocking histone deacetylation in Arabidopsis induces

pleiotropic effects on plant gene regulation and development. PNAS *98*, 200–205.

Tian, L., Fong, M.P., Wang, J.J., Wei, N.E., Jiang, H., Doerge, R.W., and Chen, Z.J. (2005). Reversible histone acetylation and deacetylation mediate genome-wide, promoter-dependent and locus-specific changes in gene expression during plant development. Genetics *169*, 337–345.

Wang, Y., Tang, shuang-qin, Wu, Z., Shi, Q., and Wu, Z. (2018). Phenotypic analysis of a dwarf and deformed flower3 (ddf3) mutant in rice (Oryza sativa L.) and characterization of candidate genes. Journal of Integrative Agriculture *17*, 1057–1065.

Watson, P.J., Fairall, L., and Schwabe, J.W.R. (2012). Nuclear hormone receptor co-repressors: Structure and function. Molecular and Cellular Endocrinology *348*, 440–449.

Wei, X., Xu, J., Guo, H., Jiang, L., Chen, S., Yu, C., Zhou, Z., Hu, P., Zhai, H., and Wan, J. (2010). DTH8 suppresses flowering in rice, influencing plant height and yield potential simultaneously. Plant Physiol. *153*, 1747–1758.

Woo, Y.-M., Park, H.-J., Su'udi, M., Yang, J.-I., Park, J.-J., Back, K., Park, Y.-M., and An, G. (2007). Constitutively wilted 1, a member of the rice YUCCA gene family, is required for maintaining water homeostasis and an appropriate root to shoot ratio. Plant Mol. Biol. *65*, 125–136.

Wu, C., Fu, Y., Hu, G., Si, H., Cheng, S., and Liu, W. (2010). Isolation and characterization of a rice mutant with narrow and rolled leaves. Planta *232*, 313–324.

Xu, D., Shi, J., Rautengarten, C., Yang, L., Qian, X., Uzair, M., Zhu, L., Luo, Q., An, G., Waßmann, F., et al. (2017). Defective Pollen Wall 2 (DPW2) Encodes an Acyl Transferase Required for Rice Pollen Development. Plant Physiology *173*, 240–255.

Yonemaru, J.-I., Choi, S.H., Sakai, H., Ando, T., Shomura, A., Yano, M., Wu, J., and Fukuoka, S. (2015). Genome-wide indel markers shared by diverse Asian rice cultivars compared to Japanese rice cultivar "Koshihikari." Breed. Sci. 65, 249–256.

Yoshida, H., and Nagato, Y. (2011). Flower development in rice. J Exp Bot *62*, 4719–4730.

Yu, J., Li, Y., Ishizuka, T., Guenther, M.G., and Lazar, M.A. (2003). A SANT motif in the SMRT corepressor interprets the histone code and promotes histone deacetylation. EMBO J. *22*, 3403–3410.

Yumul, R.E., Kim, Y.J., Liu, X., Wang, R., Ding, J., Xiao, L., and Chen, X. (2013). POWERDRESS and diversified expression of the MIR172 gene family bolster the floral stem cell network. PLoS Genet. *9*, e1003218.

Zheng, M., Wang, Y., Wang, Y., Wang, C., Ren, Y., Lv, J., Peng, C., Wu, T., Liu, K., Zhao, S., et al. (2015). DEFORMED FLORAL ORGAN1 (DFO1) regulates floral organ

identity by epigenetically repressing the expression of OsMADS58 in rice (Oryza sativa). New Phytol. *206*, 1476–1490.

Zhou, C., Zhang, L., Duan, J., Miki, B., and Wu, K. (2005). HISTONE DEACETYLASE19 is involved in jasmonic acid and ethylene signaling of pathogen response in Arabidopsis. Plant Cell *17*, 1196–1204.

Zhu, Q.-H., Ramm, K., Shivakkumar, R., Dennis, E.S., and Upadhyaya, N.M. (2004). The ANTHER INDEHISCENCE1 Gene Encoding a Single MYB Domain Protein Is Involved in Anther Development in Rice. Plant Physiol *135*, 1514–1525.

# 초록

## 생육부진 돌연변이 벼의 형질조사와 유전자 지도 작성

기후변화와 인구증가 속도에 의하여 세계인구의 주요한 식량작물인 벼의 생산량을 증가시키기 위한 유전자 기능 연구가 활발히 진행되고 있는 가운데 광을 효율적으로 이용하고 높은 수량을 이끄는 이상적인 초형에 대한 필요성은 꾸준히 증가하고 있다.

본 연구에서는 삼광벼에 MNU를 처리하여 얻어진 생육부진 현상을 보이는 돌연변이체를 실험 재료로 사용하여 표현형 특성을 검정하고, 작물생육에 결정적으로 작용하는 영양기관의 정상적인 발달을 조절하는 유전자를 동정하여 그 기능을 밝히는데 도움이 되고자 하였다.

생육부진 돌연변이체는 생육초기부터 모본에 비해 잎 형태와 키가 작아지는 현상을 보였다. 영양생장기를 지나 생식생장기로 접어들면서 생육부진이 심화되는 양상을 보였고, 생식생장기에서는 출수가 늦어지고, 수분/수정이 정상적으로 이루어 지지 않아 완전한 불임의 형태를 보였다.

돌연변이체는 모본에 비해 키가 약 34% 감소하였고, 45%의 잎 폭의 감소율을 보였다. 잎을 횡단/종단으로 절단하여 세포 크기의 변화를 관찰하였을 때 모본과 돌연변이체 사이의 유의미한 세포 크기의 변화는 나타나지 않았고, 관다발의 수가 감소한 것을 볼 수 있었다. 전체적인 형태의 차이는 보이나 세포 크기 차이는 나타나지 않는다는 점에서 돌연변이체의 왜소한 형태는 세포증식 이상으로 나타나는 현상이라고 유추할 수 있었다. 또한, 출수 이후 화분 활력을 관

찰하였을 때, 돌연변이체는 약 30% 미만의 화분 활력을 가지는 것으로 나타났고, 이로 인해 불임 현상을 보이는 것으로 생각된다.

모본과 교배한 $F_1$은 모두 모본과 같은 표현형을 보이고, $F_2$ 집단은 표현형의 분리비가 3:1로 나타났기 때문에 돌연변이 표현형은 단일열성유전자에 의해 조절되는 것을 알 수 있었다. 밀양23과 교배하여 만든 집단을 이용하여 STS, CAPS, dCAPS 마커들을 제작해 유전자 동정을 시도하였고, 5번 염색체 단완의 상단부에서 약 84kb 구간으로 후보유전자 구간을 좁혔다. 구간 내의 유전자 서열을 분석을 하여 12개의 후보 유전자들 중에서 유전자 *LOC_Os05g03550*의 3번째 exon에 추가적인 11 nucleotide가 삽입된 것을 확인하였다. 이로 인해 단백질을 번역하는 과정에서 도메인 앞에서 stop codon이 생겨 정상 기능을 하지 못하는 단백질이 만들어질 것으로 예상된다.

해당 유전자가 가지고 있는 SANT(SWI3/ADA2/N-CoR/TFIII-B) 도메인은 동물과 효모에서 전사조절인자와 함께 복합체를 형성하는 co-repressor 단백질의 특징적인 도메인으로 알려져 있다. 그리고 이에 대해 여러 전사조절 단백질들과 복합체를 이루어 염색질의 구조변화를 유도하고, 하위 유전자들의 발현을 조절한다고 밝혀진 연구결과들이 있다. 하지만 아직까지 벼에서는 그 기능이 연구된 바가 없다.

따라서 해당 실험의 결과는 차후 벼의 생육에 중요한 역할을 하는 유전자 연구에 기초 자료를 제공하는 데에 그 의의가 있다.

주요어: 벼, 생육 부진, 단간, 불임, 좁은 잎폭, 유전자지도작성, SANT도메인
학번: 2016-25286

# ACKNOWLEDGEMENT

2년의 석사과정은 저에게 많은 배움을 준 소중한 시간이었습니다. 이렇게 학위를 시작하고 마무리 할 수 있도록 이끌어주신 고희종 교수님께 진심으로 감사의 말씀을 드립니다. 그리고 제가 더 발전하는 학생이 될 수 있게 도와주신 이변우 교수님, 이석하 교수님, 백남천 교수님, 서학수 교수님, 김도순 교수님, 양태진 교수님, 그리고 김광수 교수님께도 감사의 마음을 전합니다.

그동안 저를 후배로 잘 받아주시고 챙겨주신 은별 언니, 문진석 박사님, 정환이 오빠, 동령이 오빠, 요예 언니, 길응이 오빠, 수 오빠, 키쇼르, 서우 오빠, 탁이 모두 고맙습니다. 부족한 면이 많았지만 선배들의 따뜻한 격려로 여기까지 올 수 있었습니다. 그리고 오랜 시간 함께 하지는 않았지만 저를 아껴주고 응원해주신 이춘석 박사님, 우미옥 박사님, 김백기 박사님, 박종화 박사님, 추이디 언니, 윤주 언니, 윤경이에게도 고맙습니다. 그리고 나에게 소중한 후배들, 소명이, 태준이, 유석이, 지환이 덕분에 즐거웠습니다.

농장에서 학생들이 늘 배움을 얻도록 도와주시고, 지원해주시는 김홍렬 연구관님께도 깊은 감사의 말씀을 전합니다. 학생들을 늘 편안하게 배려해주시는 강미경 여사님 감사합니다. 그리고 궂은 일도 마다 않고 도와주신 종석이 오빠와 늘 씩씩한 진우에게도 고마운 마음을 전합니다.

그리고 제가 이 자리에 있을 수 있게 기회를 주시고 용기를 주신 이주현 교수님께도 감사하다는 말씀 전하고 싶습니다.

마지막으로 뒤에서 응원해주신 우리 가족들과 그 중에서도 아낌없이 저를 지지해주고 지원해준 남편에게 사랑의 마음을 전합니다.